DOI 10.1515/dmdi-2013-0015 — Drug Metab Drug Interact 2013; 28(3): 167–176

Ana Silva, Daniel Luís, Susana Santos, Joana Silva, Ana Soraia Mendo, Lidia Coito, Telma F.S. Silva, Maria Fatima C. Guedes da Silva, Luísa M.D.R.S. Martins, Armando J.L. Pombeiro, Pedro M. Borralho, Cecília M.P. Rodrigues, Maria Guadalupe Cabral, Paula A. Videira, Carolino Monteiro and Alexandra R. Fernandes*

Biological characterization of the antiproliferative potential of Co(II) and Sn(IV) coordination compounds in human cancer cell lines: a comparative proteomic approach

Abstract

Background: The discovery of cisplatin's antitumor activity led to a great interest in the potential application of coordination compounds as chemotherapeutic agents. It is essential to identify new compounds that selectively inhibit tumor proliferation, evading secondary effects and resistance associated with chemotherapeutics.

Methods: The *in vitro* antiproliferative potential of an organotin(IV) compound was evaluated using colorectal and hepatocellular carcinoma, mammary gland adenocarcinoma cell lines, and human fibroblasts. Tumor cell death was evaluated by fluorescence microscopy and flow cytometry for the Sn(IV) compound and also for a Co(II) compound bearing 1,10-phenanthroline-5,6-dione as ligand. Comparative proteomic analysis for both compounds was assessed in the colorectal cancer cell line.

Results: The Sn(IV) compound presented a high cytotoxic effect in colorectal and hepatocellular carcinoma cell lines (IC_{50} of 0.238±0.011 μM, 0.199±0.003 μM, respectively), and a lower cytotoxicity in human fibroblasts. Both compounds induced cell apoptosis and promoted the overexpression of oxidative stress-related enzyme superoxide dismutase [Cu-Zn] (SODC). The Co(II) compound induced a decreased expression of anti-apoptotic proteins (translationally-controlled tumor protein and endoplasmin), and the Sn(IV) compound decreased expression of proteins involved in microtubule stabilization, TCTP, and cofilin-1.

Conclusions: Our data reveals a high *in vitro* antiproliferative potential against cancer cell lines and a moderate selectivity promoted by the Sn(IV) compound. Proteomic analysis of Sn(IV) and Co(II) compounds in the colorectal cancer cell line allowed an insight to their mechanisms of action, particularly by affecting the expression of proteins typically deregulated in cancer, and also suggesting a promising therapeutic potential for both compounds.

Keywords: cancer cell lines; Co(II) coordination compound; microtubule stabilization; organotin(IV) coordination compound; oxidative stress; proteomics.

Ana Silva, Daniel Luís, Susana Santos contributed equally to this work.
***Corresponding author: Alexandra R. Fernandes,** Departamento Ciências da Vida, Faculdade de Ciências e Tecnologia, Caparica, Portugal, E-mail: alexandrancrfernandes@gmail.com; and Centro de Química Estrutural, Complexo I, Instituto Superior Técnico, Lisbon, Portugal
Ana Silva and Daniel Luís: Faculdade de Engenharia, Universidade Lusófona de Humanidades e Tecnologias, Lisbon, Portugal; and Department of Biochemistry and Human Biology, Faculty of Pharmacy, University of Lisbon, Lisbon, Portugal
Susana Santos: Faculdade de Engenharia, Universidade Lusófona de Humanidades e Tecnologias, Lisbon, Portugal; Department of Biochemistry and Human Biology, Faculty of Pharmacy, University of Lisbon, Lisbon, Portugal; Centro de Química Estrutural, Complexo I, Instituto Superior Técnico, Technical University of Lisbon, Lisbon, Portugal
Joana Silva, Ana Soraia Mendo and Lidia Coito: Faculdade de Engenharia, Universidade Lusófona de Humanidades e Tecnologias, Lisbon, Portugal
Telma F.S. Silva and Luísa M.D.R.S. Martins: Centro de Química Estrutural, Complexo I, Instituto Superior Técnico, Technical University of Lisbon, Lisbon, Portugal; and Area Departamental de Engenharia Química, ISEL, Lisbon, Portugal
Maria Fatima C. Guedes da Silva: Faculdade de Engenharia, Universidade Lusófona de Humanidades e Tecnologias, Lisbon, Portugal; and Centro de Química Estrutural, Complexo I, Instituto Superior Técnico, Technical University of Lisbon, Lisbon, Portugal
Armando J.L. Pombeiro: Centro de Química Estrutural, Complexo I, Instituto Superior Técnico, Technical University of Lisbon, Lisbon, Portugal
Pedro M. Borralho and Cecília M.P. Rodrigues: Department of Biochemistry and Human Biology, Faculty of Pharmacy, University of Lisbon, Lisbon, Portugal; and Research Institute for Medicine and Pharmaceutical Sciences (iMed.UL), Faculty of Pharmacy, University of Lisbon, Lisbon, Portugal
Maria Guadalupe Cabral: Faculdade de Engenharia, Universidade Lusófona de Humanidades e Tecnologias, Lisbon, Portugal; and

CEDOC, Faculdade de Ciências Médicas, Universidade Nova de Lisboa, Lisbon, Portugal
Paula A. Videira: CEDOC, Faculdade de Ciências Médicas, Universidade Nova de Lisboa, Lisbon, Portugal
Carolino Monteiro: Department of Biochemistry and Human Biology, Faculty of Pharmacy, University of Lisbon, Lisbon, Portugal; and CENCIFOR, Coimbra, Portugal

Introduction

In the last few years, a great effort has been put forward in cancer drug discovery to develop new molecules that can effectively inhibit cancer cell proliferation without promoting the undesirable side effects that limit the efficacy of cancer therapy [1]. Despite that, effective therapies for most tumor types are lacking and cancer is still a leading cause of death worldwide [2]. The field of medicinal inorganic chemistry was powered by the discovery of cisplatin, which was approved for clinical use by the US Food and Drug Administration (FDA) in 1978 [3]. Specifically, it was the cytotoxicity to healthy cells and the tumor resistance to cisplatin, either acquired or intrinsic, that triggered the synthesis of a great number of cisplatin analogues, in an effort to develop safer and more effective platinum-based cancer therapy [4]. Furthermore, there is also a great interest in non-platinum based metallodrugs in order to exploit new molecular mechanisms of action that are effective against cells with acquired resistance to platinum drugs [5]. Here, we present two non-platinum coordination compounds: a cyclic trinuclear complex of Sn(IV) bearing an aromatic oximehydroxamic acid group $[nBu_2Sn(L)]_3(H_2L$=N,2-dihydroxy-5-[N-hydroxyethanimidoyl] benzamide) [6] (Figure 1A) and a Co(II) compound bearing 1,10-phenanthroline-5,6-dione (phendione) $[Co(Phendione)_2(H_2O)Cl]BF_4$ [7] (Figure 1B).

Oximehydroxamic acid was selected as a ligand regarding the antitumor potential displayed by organotin compounds bearing hydroxamate ligands [8]. Phenanthrolines are also versatile ligands with interesting biological properties, such as the redox activity of some derivatives [9] and their planar structure, which promotes the interaction with nucleic acids [10]. In fact, it is known that the ability of complexes bearing the ligand phendione is to bind covalently to both proteins [11] and DNA [12], whereas the Co^{2+} ion was demonstrated to promote apoptosis in human macrophages [13]. The cytotoxicity of these two compounds was previously tested by our group in several tumor cell lines, and both presented very high *in vitro* cytotoxicity [6, 7]. Specifically, the Sn(IV) compound proved to have high *in vitro* tumor-inhibiting activity in human promyelocytic leukemia (HL-60), hepatocellular carcinoma (Bel-7402), gastric carcinoma (BGC-823), and nasopharyngeal carcinoma (KB) cell lines [6]. Whereas the Co(II) compound was shown to be highly cytotoxic to HCT116, HepG2, and MCF-7 tumor cell lines [7]. We focused our work on the evaluation of the *in vitro* antiproliferative potential of the Sn(IV) compound against HCT116, HepG2, and MCF-7 tumor cell lines in comparison to human healthy fibroblasts. The primary cellular targets and the biochemical pathways affected by these compounds were evaluated by comparative proteomic analysis, a technology proven to be very useful to explore the molecular

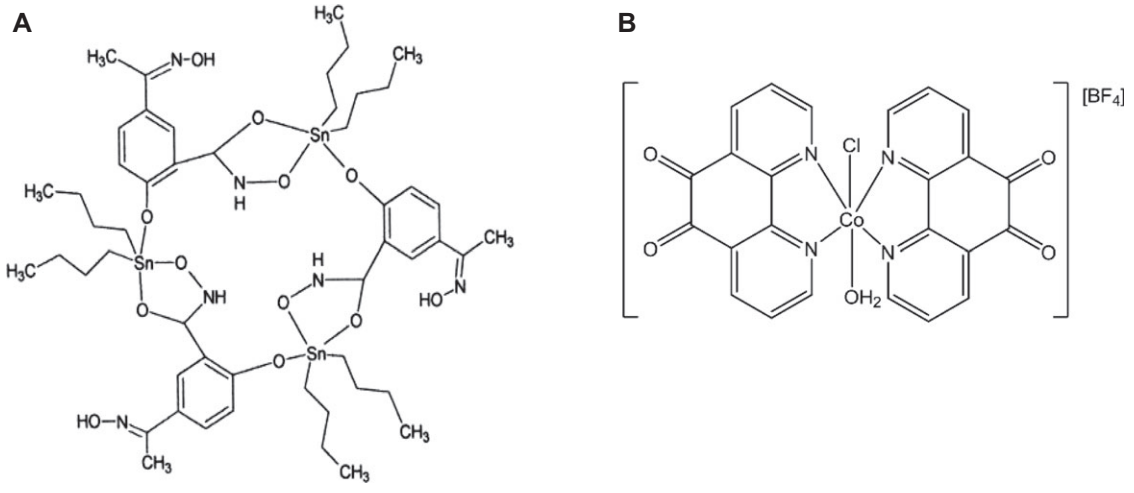

Figure 1 Chemical structure of the Sn(IV) (A) and Co(II) (B) coordination compounds.

mechanisms of antitumor drugs [14–16], particularly in the study of chemoresistance pathways [17–22], and evaluation of altered protein expression patterns resulting from drug treatment [23]. These altered patterns can provide insights into drug activity and cytotoxicity, and allows the prediction of side effects resulting from off-target interactions [15]. In this work the mechanisms underlying HCT116 tumor cell death in the presence of the two coordination compounds gained new insights as 2-dimensional gel electrophoresis (2-DE) based proteomics allowed the detection of altered protein expression patterns, associated with pathways related to compound exposure/activity.

Materials and methods

Cell culture

HCT116 human colorectal carcinoma and HepG2 human hepatocellular carcinoma cell lines were grown as previously described [24]. MCF-7 cells were derived from pleural effusion of breast adenocarcinoma from a female patient and were grown in the same conditions and medium as HepG2 cells. This cell line was kindly provided by António Sebastião Rodrigues (Human Molecular Genetics Research Centre (CIGMH), Department of Genetics, Faculty of Medical Sciences, New University of Lisbon, Lisbon, Portugal). Normal human fibroblasts were grown in the same conditions as HepG2 and MCF-7 cell lines and were kindly provided by Isabel Carreira (Laboratory of Cytogenetics and Genomics, Faculty of Medicine, University of Coimbra, Coimbra, Portugal).

Cell viability

Cells were plated at 5000 cells/well in 96 well plates. Media was removed 24 h after platting and replaced with fresh media containing 0.1–10 μM of Sn(IV) compound or 0.1% (v/v) ethanol (vehicle control). These solutions were prepared from 1000 times concentrated stock solutions of the complex to assure a maximum volume of ethanol in culture medium of 0.1% (v/v). After 48 h of cell incubation in the presence or absence of each compound, cell viability was evaluated with CellTiter 96® AQueous non-radioactive cell proliferation assay (Promega, Madison, WI, USA), as described in [24].

Hoechst 33258 labeling

HCT116 cells were plated in 35 mm dishes at 150,000 cells/dish. Culture medium was removed 24 h after platting and replaced with 2 mL of fresh medium containing either 0.20 μM Sn(IV) compound or 0.1% (v/v) ethanol (vehicle control) and 0.35 μM Co(II) compound or sterile water (vehicle control). Cells treated with Co(II) compound were stained after an incubation period of 20 h and 48 h, whereas those incubated with Sn(II) compound were stained after 48 h. Hoechst staining assay was performed as described in [24].

Cell death by flow cytometry

HCT116 cells were seeded into 35 mm dishes at 150,000 cells/dish. Culture medium was removed 24 h after platting and replaced with 2 mL of fresh medium containing either 0.20 μM Sn(IV) compound, 0.20 μM, and 0.35 μM Co(II) compound or sterile water (vehicle control). Cells were incubated in the presence of each compound for 48 h and then stained with propidium iodide (PI) and fluorescein isothiocyanate (FITC) labeled Annexin V according to the manufacturer's instructions (Annexin V-FITC apoptosis detection kit; Invitrogen, Carlsbad, CA, USA). Briefly, both floating and adherent cells were collected, rinsed twice with cold phosphate buffered saline (PBS) 1× (Invitrogen) and re-suspended in 100 μL of 1× annexin binding buffer. Annexin V-FITC and PI were added according to manufacturer's directions and samples were incubated in the dark for 15 min; 400 μL of 1× annexin binding buffer was added to each sample. Data were collected on a BD FACSCalibur flow cytometer using CellQuest software (Becton Dickinson, Franklin Lakes, NJ, USA) and analyzed with Paint-a-Gate software (Becton Dickinson).

Protein sample preparation

HCT116 cells were seeded into 25 cm^2 culture flasks at 6×10^5 cells/flask. Culture medium was removed 24 h after platting and replaced with fresh medium containing 0.20 μM of either Sn(IV)- or Co(II)-compound or their respective solvents: 0.1% (v/v) ethanol and sterile water (vehicle controls). Cells were incubated in the presence of each compound for 48 h and collected for protein extraction. In order to minimize sample degradation, all solutions for sample preparation contained 1× phosphatase inhibitor (PhosStop, Roche, Basel, Switzerland), 1× protease inhibitor (complete Mini, Roche®), 1 mM PMSF and 0.1% (w/v) dithiothreitol. Collected cells were concentrated in lysis buffer (150 mM NaCl; 50 mMTris, pH 8.0; 5 mM EDTA, 2% (w/v) NP-40) by centrifugation at 14,000 *g* for 30 min at 4°C. Supernatant was collected and samples stored at –80°C.

Two-dimensional gel electrophoresis

Two-dimensional gel electrophoresis was performed as described in [25]. Prior to 2-DE, protein concentration was determined via the 2-D Quant kit (GE Healthcare, Little Chalfont, UK). Isoelectric focusing (IEF) was performed using Immobilized pH gradient (IPG) strips (7 cm long IPG strips covering pH range from 3–10; GE Healthcare®) in an EttanIPGphor 3 focusing unit (GE Healthcare®) [25]. All 2-DE gel images were digitalized (PIXMA M250; Canon, Uxbridge, UK) and analyzed with the Melanie 7.0 Software (GeneBio, Geneva, Switzerland). Each one of the conditions studied was evaluated in triplicate. The analysis was performed semi-automatically by the software, adhering to the following procedure: (i) spot detection; (ii) spot matching from different gels; (iii) background subtraction; and (iv) assessment of the normalized intensity of each spot. Normalization was performed as the ratio of the spot intensity and the total intensity of

the spots with a match in all gels in the experiment. Variation of each protein expression level was calculated as the ratio of the normalized intensity of each protein spot in gels corresponding to each condition compared to those corresponding to control samples. The Mr value for each identified protein was determined by comparison with the relative positions of the proteins included in the molecular weight protein marker (HyperPAGE, Bioline, London, UK), which was run for the second dimension simultaneously with the samples under study. Spots with significantly altered intensities between conditions (up or down-regulated peptides in comparison to control samples) were selected and picked from gels towards identification through MALDI-TOF mass spectrometry.

In-gel digestion and MALDI-TOF mass spectrometry analysis

Selected protein spots were manually excised from 2-DE gels and sent for peptide mass fingerprinting analysis at the Mass Spectrometry Laboratory in ITQB/iBET (paid service, Oeiras, Portugal).

Detection of reactive oxygen species (ROS)

Cellular ROS generation was examined by using 2,7-dichlorodihydrofluorescein diacetate (H_2DCF-DA) (Invitrogen). DCFH-DA is a nonpolar dye, converted into the polar derivative DCFH by cellular esterases that are nonfluorescent but switched to highly fluorescent DCF when oxidized by intracellular ROS and other peroxides to yield the highly fluorescent 2′,7′-dichlorofluorescein (DCF); HCT116 cells were seeded into 25 cm^2 culture flasks at 6×10^5 cells/flask. Culture medium was removed 24 h after platting and replaced with fresh medium containing 0.20 μM of each compound, 0.1% (v/v) ethanol or sterile water (vehicle controls). Hydrogen peroxide at a concentration of 100 μM was used as a positive control. After 48 h at 37°C and 5% (v/v) CO_2 cells were harvested and washed with PBS. Cells were re-suspended in pre-warmed PBS containing 10 μM H_2DCF-DA and incubated at 37°C for 20 min. Production of ROS, based on the levels of DCF positive cells was analyzed by flow cytometry in an Attune cytometer (Applied Biosystems, Foster City, CA, USA) and analyzed with the Attune Cytometric Software (Applied Biosystems).

Cell cycle analysis

Cells were seeded in 25 cm^2 culture flasks with a density of 0.75×10^5 cells/mL and were synchronized in early S-phase by a double thymidine block, as previously described [26]. Cells were release from the second block by substituting the medium with 2 mM thymidine (Sigma, St Louis, MO, USA) for fresh medium without thymidine and either with 0.2 μM of Co(II) compound or sterile water (vehicle control). After incubation periods of 4 h and 8 h at 37°C and 5% CO_2 the media was removed and cells were trypsinised, transferred to microtubes, harvested by centrifugation (1000 *g* for 5 min) and washed with PBS 1×. Cell pellet was resuspended in 1 mL of cold PBS 1× and 1 mL of cold 80% ethanol was added drop by drop to each tube while gently vortexing. Cell suspension was kept in ice for 30 min and stored at 4°C for at least 14 h. Cells were pelleted, resuspended in 50 μg/mL RNase A in PBS 1× and incubated at 37°C for 30 min. PI was added to a final concentration of 2.5 μg/mL and DNA content was analyzed on a BD FACSCalibur Flow Cytometer (Becton Dickinson).

Statistical analysis

All data were expressed as mean±SEM from at least three independent experiments. Statistical significance was evaluated using the Student's t-test; $p<0.05$ was considered statistically significant.

Results and discussion

The *in vitro* antiproliferative potential of the Sn(IV) compound was evaluated in HCT116, HepG2 and MCF-7 tumor cell lines and human normal fibroblasts employing the spectrophotometrical quantification of formazan that resulted from the reduction of MTS by cells with active mitochondrial dehydrogenases, using the CellTiter 96® AQueous non-radioactive cell proliferation assay. The *in vitro* cytotoxicity was expressed as the concentration of compound that inhibits proliferation of cells by 50% as compared to untreated cells (IC_{50}; μM). A decrease of the cell viability, in a dose-dependent manner, was observed for the Sn(IV) compound in all cell lines (Figure 2). Nevertheless, the compound was more active against

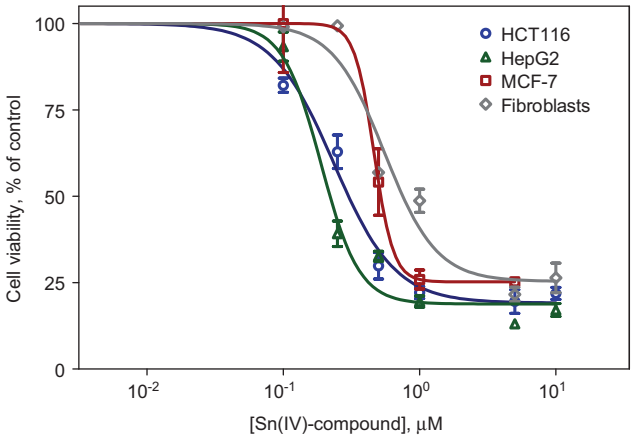

Figure 2 Dose-dependent cytotoxicity of the Sn(IV)-compound in HCT116 cells (dark blue), HepG2 cells (dark green), MCF-7 cells (brown), and fibroblasts (gray).
Cells were incubated in the presence of the complex for 48 h and their viability was evaluated by MTS metabolization. Dose-response curve and the corresponding IC_{50} were calculated by nonlinear regression analysis using GraphPad Prism (Graph Pad Software Inc., San Diego, CA, USA). The results are expressed as the mean±SEM percentage compared to controls from three independent experiments.

malignant cell lines (Figure 2). The IC_{50} values determined for malignant cell lines were 0.238±0.011 μM (HCT116), 0.199±0.003 μM (HepG2) and 0.477±0.019 μM (MCF-7) (Table 1). Indeed, the Sn(IV) compound is approximately 2.3 and 2.7 times more active against HCT116 and HepG2 cells, respectively, compared to normal fibroblasts (IC_{50} of 0.538±0.047 μM), indicating some *in vitro* selectivity for colorectal and hepatocellular tumor cell lines (Figure 2; Table 1). The Co(II) compound bearing 1,10-phenanthroline-5,6-dione also presented high antitumor activity towards HCT116, HepG2 and MCF-7 cells (IC_{50} values of 0.206±0.023 μM, 0.582±0.034 μM, and 0.690±0.246 μM, respectively), as previously demonstrated by our group [7]. This compound also displays some selectivity for colorectal cancer cells compared to human fibroblasts (IC_{50} 0.62±0.01), being approximately 3 times more active against the HCT116 tumor cell line (Table 1) [7].

Nuclear staining with Hoechst 33258 was used to evaluate the effects in nuclear morphology in result of cell exposure to each compound (Figure 3). Regarding the effect of the Co(II)-compound, cells were first treated for 48 h. However, despite the lower cell density comparing to the vehicle control, a reduced number of apoptotic nuclei were observed (Figure S1, which accompanies the article at http://www.degruyter.com/view/j/dmdi.2013.28.issue-3/issue-files/dmdi.2013.28.issue-3.xml). For this reason the exposure period for the Co(II)-compound was reduced to 20 h (Figure 3C, D).

The majority of solvent-treated HCT116 cells (vehicle controls) presented nuclei with homogeneous distribution of fluorescence, indicating the presence of uncondensed chromatin dispersed through the whole nucleus (Figure 3A, C), which is representative of viable interphase cells [27]. Cells undergoing mitosis were also observed. On

Table 1 IC_{50} values for Sn(IV) and Co(II)-compounds on human colorectal (HCT116), hepatocellular (HepG2) and breast (MCF-7) carcinoma cell lines and human fibroblasts.

Cell line	IC_{50} (±SEM) μM				Reference
	HCT116	HepG2	MCF-7	Fibroblasts	
Sn(IV)-compound	0.238 (±0.011)	0.199 (±0.003)	0.477 (±0.019)	0.538 (±0.047)	Present work
Co(II)-compound	0.206 (±0.023)	0.582 (±0.034)	0.69 (±0.25)	0.611 (±0.008)	[7]

The results are expressed as mean±SEM from at least three independent experiments.

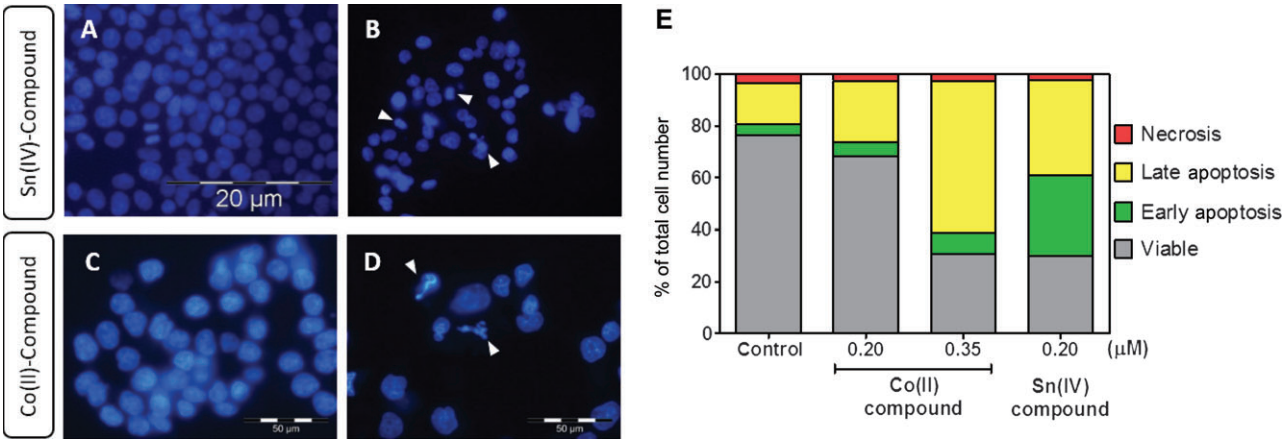

Figure 3 Morphological alterations of the nucleus resulting from exposure of HCT116 cells to 0.20 μM Sn(IV)-compound for 48 h (B) and 0.35 μM Co(II)-compound for 20 h (D) compared to their respective solvent controls: 0.1% (v/v) ethanol (A) and sterile water (C). Nuclei stained with DNA-specific dye Hoechst 33258. White arrowheads indicate major alterations in nuclear morphology such as chromatin condensation and nuclear fragmentation. (E) Proportion of apoptotic and necrotic cell death in solvent (vehicle control) and compound-treated HCT116 cells.

Cells were incubated with increasing concentrations of each one of the coordination compounds for a period of 48 h. Cell death was determined by flow cytometry after Annexin-V/fluorescein isothiocyanate (FITC) and propidium iodide (PI) double staining.

Gray, viable cells; green, early apoptosis; yellow, late apoptosis; red, necrosis.

the contrary, two nuclear morphological alterations typically associated with apoptosis could be observed in cells treated with each one of the studied complexes, namely chromatin condensation and nuclear fragmentation [28], as indicated by the bright non-homogeneous fluorescence (Figure 3B, D; white arrowheads).

Double staining with PI and Annexin V-FITC was used to distinguish between apoptotic and necrotic cell death, as Annexin V binds specifically to externalized phosphatidylserine, and PI only penetrates in cells with damaged membranes. In the presence of 0.20 μM Co(II)-compound, the number of apoptotic cells, either in early ($FITC^+/PI^-$) and later stages ($FITC^+/PI^+$), almost doubled compared to the vehicle control, reaching a 3.3-fold change (the highest obtained value) for a concentration of 0.35 μM (Figure 3E). Sn(IV)-compound at 0.20 μM induced a similar proportion of apoptotic cells when compared with 0.35 μM of Co(II)-compound, demonstrating a higher ability to promote apoptosis than the latter (Figure 3E). However, most of the apoptotic cells that resulted from Co(II)-compound exposure presented PI-permeable membranes by contrast with those treated with Sn(IV)-compound. The higher proportion of cells on later stages of apoptosis is indicative that the former may be able to induce apoptosis more readily, thus, presenting a potentially faster mechanism of action. The presence of both coordination compounds did not result in an increase of necrotic cells (Figure 3E). Interestingly, the number of cells that were undergoing necrosis is even lower than that observed for untreated samples (Figure 3E).

In an effort to further characterize the molecular mechanisms underlying the biological activity of the coordination compounds here described, variation of protein expression levels as a cellular response to the presence of each compound were analyzed through comparative proteomics (Figure S2). All proteins that were identified by MALDI-TOF-MS are listed on Table S1, and those whose expression levels varied more significantly between compound-treated cells and respective vehicle-treated (control) cells are listed in Table 2.

When HCT116 cells were exposed to the Co(II) compound an overexpression of oxidative stress-related enzymes, superoxide dismutase [Cu-Zn] (SODC) and peroxiredoxine 2 (PRDX2), and of stratifin (14-3-3 protein σ), and the proliferation-associated protein 2G4 (PA2G4) was observed (Figure S2A, B; Table 2). Contrary, a decrease of the expression levels of the translationally-controlled tumor protein (TCTP), the heat shock protein beta 1 (HSPB1), the endoplasmin (HSP90B1), and the cytoskeleton-related proteins, tropomyosin 3 (TPM3), and ezrin (EZRI) was found (Figure 3A, B; Table 1). PRDX2 and SODC are two antioxidant enzymes whose expression is induced by oxidative damage [29]. These proteins protect cells from reactive oxygen species (ROS) by reducing peroxides and the superoxide anion, respectively [29]. The formation of such highly reactive oxidizing molecules might arise from the redox properties of the Co(II) compound. Indeed, when we exposed HCT116 cells to the Co(II) compound, an increased level of ROS was observed (66% of DCF

Table 2 Proteome evaluation: MALDI-TOF mass spectrometry. Proteins whose expression levels were significantly altered (more than 1.5-fold) after 24 h of exposure of HCT116 cells to 0.20 μM of each coordination compound.

Spot ID	Protein identification[a]	Protein reference (HUMAN)	Co(II) compound	Sn(IV) compound
1	Peptidyl-prolyl cis-trans isomerase A	PPIA	NA	−4.21
3	Heat shock protein β-1	HSPB1	−1.61	NA
5	Peroxiredoxin-2	PRDX2	2.08	NA
6	Superoxide dismutase [Cu-Zn]	SODC	2.18	1.50
8	Galectin-1	LEG1	NA	−1.87
10	Translationally-controlled tumor protein	TCTP	−1.57	−2.02
13	Complement component 1 Q subcomponent-binding protein, mitochondrial	C1QBP	NA	−1.56
14	Tropomyosin α-3 chain	TPM3	−2.01	NA
15	Stratifin/14-3-3 protein σ	1433S	1.50	NA
17	Voltage-dependent anion-selective channel protein 1	VDAC1	NA	1.57
19	Profilin-1	PROF1	NA	1.63
20	Cofilin-1	COF1	NA	−1.97
22	Endoplasmin	HSP90B1/GPR94	−1.54	NA
23	Proliferation-associated protein 2G4	PA2G4	1.71	NA
24	Ezrin	EZRI	−2.04	NA

NA, protein expression levels not significantly altered in comparison to control gels. [a]http://www.uniprot.org/.

positive cells compared with 14% in untreated HCT116 cells) (Figure 4) as a result of an increase of the highly fluorescent DCF when oxidized by intracellular ROS. The incubation of HCT116 cells for 48 h to H_2O_2 (100 μM), an oxidant compound known to induce ROS, showed 44% of DCF positive cells demonstrating the higher levels of ROS produced by the Co(II) compound (Figure 4).

PA2G4 is involved in growth regulation and its overexpression was found to inhibit the proliferation of fibroblasts and cancer cells [30, 31]. Similarly, 14-3-3σ have also been extensively related to cell growth control by inhibiting cell cycle progression [32, 33]. Thus, the elevated levels of PA2G4 and 14-3-3σ indicate that the Co(II) compound might interfere with the progression of cell cycle and this hypothesis was also validated by our group (Figure 5). As we can observe in Figure 5, the Co(II) compound induce a cell cycle arrest avoiding cells to enter in G2/mitosis. Indeed, most of HCT116 cells at 4 h and at 8 h of Co(II) compound exposure are at S-phase while untreated cells have progressed to G2/mitosis (Figure 5A, B).

TCTP, a highly conserved polypeptide with anti-apoptotic and growth-promoting properties [34] was recently suggested to exert its anti-apoptotic activity by destabilizing the tumor suppressor protein p53 [34]. Indeed, its ability to act as a survival factor is corroborated by the induction of apoptosis after gene silencing by siRNA [35]. Also, HSPB1 overexpression is associated with several types of cancers, poor outcome, and chemoresistance [36–38]. As such, TCTP and HSPB1 may be considered therapeutic targets and the ability of the Co(II) compound to induce the decrease of their expression levels is suggestive

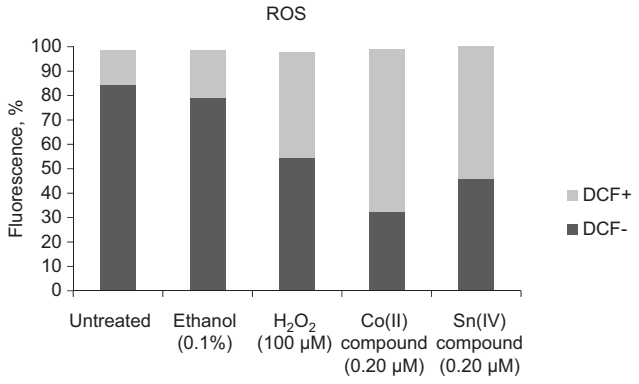

Figure 4 Reactive oxygen species (ROS).
Percentage of DCF positive (DCF+) and DCF negative (DCF–) cells in water or 0.1% (v/v) ethanol (vehicle controls) and compound-treated HCT116 cells. Cells were incubated in the absence or presence (0.2 μM) of both compounds for a period of 48 h. DCF fluorescent levels were determined by flow cytometry. H_2O_2 was used as a positive control for ROS induction.

of the potential antitumor properties of this compound. HSP90B1 is also associated with an anti-apoptotic role, apart from its function in the processing and transport of secreted proteins [39]. Up-regulation of HSP90B1 was found in esophagus adenocarcinoma [40], poorly differentiated lung cancer [41], and gastric carcinoma [42]. Thus, the decrease of this protein expression as the result of HCT116 cells treatment with the Co(II) compound is a positive feature that may contribute to its antiproliferative potential. Furthermore, the decreased expression levels of cytoskeleton-associated proteins, TPM3 and EZRI indicate the negative effect of this compound on cellular structure, as they are implicated in the stabilization of the actin filaments and their interaction with plasma membrane [43].

Concerning the effect of the Sn(IV) compound on the proteome of HCT116 cells, we found a significant overexpression of the voltage-dependent anion-selective channel protein 1 (VDAC1), of the SODC protein and of the profilin-1 protein (PROF1) (Figure 4C, D; Table 2). In order to confirm the overexpression of SODC protein, the levels of ROS were also accessed in HCT116 cells incubated in the presence (0.2 μM) or absence (0.1% (v/v) ethanol; vehicle control) of the Sn(IV) compound (Figure 4). As observed in Figure 4, there are more than 54% of positive DCF cells when these cells were incubated in the presence of this compound compared with cells incubated for the same period of time in the presence of the solvent (20%).

However, a decrease of the expression levels were observed for the complement 1q-binding protein (C1QBP), the galectin-1 protein (LEG1), the translationally-controlled tumor protein (TCTP), the peptidyl-prolyl cis-trans isomerase A protein (PPIA), and the cofilin-1 protein (COF1) (Figure 4C, D; Table 2) when cells were exposed to the Sn(IV) compound. VDAC1 has been described as an important player in the function of the mitochondria during apoptotic cell death, being involved in the release of cytochrome *c* to the cytosol [44]. The overexpression of this mitochondrial outer membrane channel is in accordance with our flow cytometry results that demonstrate the ability of the Sn(IV) to induce apoptosis in HCT116 cells (Figure 3). The mitochondrial protein, C1QBP, is also implicated in cell apoptosis, but conversely to VDCA it promotes resistance to cell death [45]. This protein is also associated with the promotion of cell migration and is reported to be up-regulated in cancer [45, 46]. Similarly, LEG1 and PPIA are found to be up-regulated in cancer cells and to contribute to several mechanisms related to tumor transformation and growth [47–50]. As such, these two proteins can be considered potential therapeutic targets and we consider their down-regulation as the result of the exposure to the Sn(IV) compound a positive

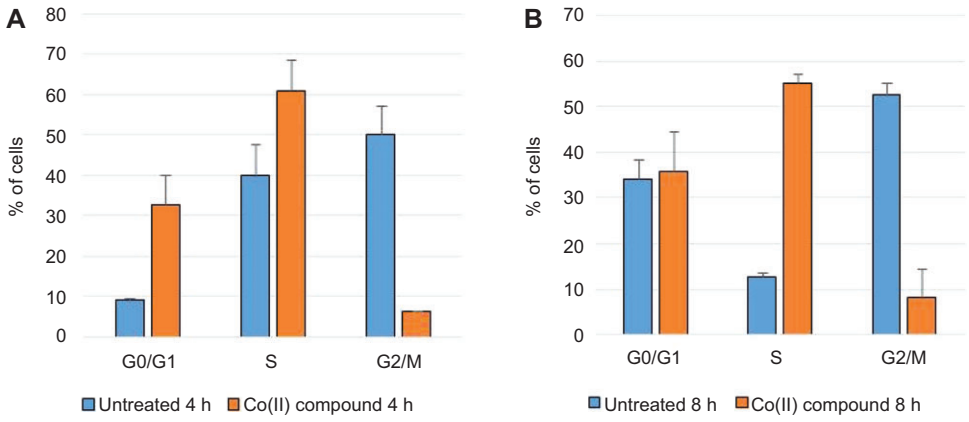

Figure 5 Cell cycle evaluation.
Percentage of HCT116 cells in the different phases of the cell cycle after incubation for 4 h (A) and 8 h (B) in the presence (0.2 μM) or absence (water) of Co(II) compound. Propidium iodide (PI) fluorescent levels were determined by flow cytometry. The results are expressed as the mean±SEM percentage from three independent experiments.

characteristic to be further explored. The same holds true for the induced overexpression of PROF1. This protein was found by others to present tumor suppressor activity, as the phenotype of cancer cells with down-regulated expression of PROF1 is reverted to a nontumorigenic state by up-regulating its levels [51]. The anti-apoptotic TCTP, which is also involved in the stabilization of microtubules and whose decrease of expression was induced by the Co(II) compound, is also down-regulated in the presence of the Sn(IV) compound. This result, together with the decrease of expression of COF1, which regulates tubulin depolymerization, may suggest that the Sn(IV) can cause an impairment in tubulin dynamics. These results are currently being validated by our group.

Conclusions

Advances in cancer treatment continue to be limited by the identification of unique cellular and biochemical aspects of each tumor. Those characteristics once profiled can be exploited to selectively target tumor cells. The recent advances in genomics and proteomics have allowed the test of several new compounds with antiproliferative potential. The Sn(IV) compound presented very high *in vitro* antiproliferative potential against human cancer cell lines, namely HCT116, HepG2, and MCF-7 (Figure 2; Table 1). Additionally, this compound shows lower cytotoxicity in healthy human fibroblasts, particularly when compared to HCT116 and HepG2 cells, thus demonstrating some selectivity for these cancer cell lines (Figure 2; Table 1). Both Sn(II) and Co(II) compounds demonstrate the ability to promote apoptosis, as demonstrated by the altered nuclear morphology, typical of apoptotic cell death, and by flow cytometry (Figure 3). Exposure of HCT116 cells to both compounds resulted in the up-regulation of SODC and this up-regulation was correlated with the higher levels of ROS in HCT116 cells exposed to both compounds (Figure 4). Exposure of HCT116 cells to both compounds also resulted in the down-regulation of proteins that were found to be up-regulated in cancer cells, namely HSPB1, GRP94, TCTP, C1QBP, LEG1, and PPIA (Figure S2; Table 2). On the contrary, the anti-proliferative PA2G4 and the apoptosis-related VDCA were found to be over-expressed in the presence of the Co(II) and the Sn(IV) compounds, respectively (Figure S2; Table 2). Indeed, Co(II) compound was shown to induce cell cycle arrest in S-phase (Figure 5). Hence, our results are suggestive that both coordination compounds presented here exhibit good therapeutic potential, affecting the expression of proteins typically deregulated in tumors. Moreover, we found a possible role of Sn(IV) in tubulin microtubules destabilization and of the Co(II) compound in the induction of oxidative stress.

Conflict of interest statement

Authors' conflict of interest disclosure: The authors stated that there are no conflicts of interest regarding the publication of this article.
Research funding: None declared.
Employment or leadership: None declared.
Honorarium: None declared.

Received March 5, 2013; accepted May 29, 2013; previously published online June 26, 2013

References

1. Blasina A, Hallin J, Chen E, Arango ME, Kraynov E, Register J, et al. Breaching the DNA damage checkpoint via PF-00477736, a novel small-molecule inhibitor of checkpoint kinase 1. Mol Cancer Ther 2008;7:2394–404.
2. Jemal A, Bray F, Center MM, Ferlay J, Ward E, Forman D. Global cancer statistics. CA Cancer J Clin 2011;61:69–90.
3. McWhinney SR, Goldberg RM, McLeod HL. Platinum neurotoxicity pharmacogenetics. Mol Cancer Ther 2009;8:10–6.
4. Kelland L. The resurgence of platinum-based cancer chemotherapy. Nat Rev Cancer 2007;7:573–84.
5. Ott I, Gust R. Non platinum metal complexes as anti-cancer drugs. Arch Pharm 2007;340:117–26.
6. Gajewska M, Luzyanin KV, Guedes da Silva MF, Li QS, Cui JR, Pombeiro AJ. Cyclic trinuclear diorganotin(IV) complexes – the first tin compounds bearing oximehydroxamate ligands: synthesis, structural characterization and high in vitro cytotoxicity. Eur J Inorg Chem 2009;2009:3765–9.
7. Silva TF, Smoleński P, Martins LM, Guedes da Silva MF, Fernandes AR, Luis D, et al. Cobalt and zinc compounds bearing 1,10-phenantroline-5,6-dione or the 1,3,5-triaza-7-phosphaadamantane derivatives – synthesis, characterization, cytotoxicity and selectivity studies. Eur J Inorg Chem 2013; DOI: 10.1002/ejic.201300197.
8. Li Q, da Silva MF, Pombeiro AJ. Diorganotin(IV) derivatives of substituted benzohydroxamic acids with high antitumor activity. Chemistry 2004;10:1456–62.
9. Wu Q, Maskus M, Pariente F, Tobalina F, Fernandez VM, Lorenzo E, et al. Electrocatalytic oxidation of NADH at glassy carbon electrodes modified with transition metal complexes containing 1,10-phenanthroline-5,6-dione ligands. Anal Chem 1996;68:3688–96.
10. Accorsi G, Listorti A, Yoosaf K, Armaroli N. 1,10-phenanthrolines: versatile building blocks for luminescent molecules, materials and metal complexes. Chem Soc Rev 2009;38:1690–700.
11. Yokoyama K, Asakura T, Nakamura N, Ohno H. Chemical modification of cytochrome c by a ruthenium complex containing phenanthroline quinone. Inorg Chem Commun 2006;9:281–3.
12. Ghosh S, Barve AC, Kumbhar AA, Kumbhar AS, Puranik VG, Datar PA, et al. Synthesis, characterization, X-ray structure and DNA photocleavage by cis-dichloro bis(diimine) Co(III) complexes. J Inorg Biochem 2006;100:331–43.
13. Petit A, Mwale F, Zukor DJ, Catelas I, Antoniou J, Huk OL. Effect of cobalt and chromium ions on bcl-2, bax, caspase-3, and caspase-8 expression in human U937 macrophages. Biomaterials 2004;25:2013–8.
14. Muroi M, Kazami S, Noda K, Kondo H, Takayama H, Kawatani M, et al. Application of proteomic profiling based on 2D-DIGE for classification of compounds according to the mechanism of action. Chem Biol 2010;17:460–70.
15. Sleno L, Emili A. Proteomic methods for drug target discovery. Curr Opin Chem Biol 2008;12:46–54.
16. Chen ST, Pan TL, Tsai YC, Huang CM. Proteomics reveals protein profile changes in doxorubicin-treated MCF-7 human breast cancer cells. Cancer Lett 2002;181:95–107.
17. Lu JJ, Chen SM, Ding J, Meng LH. Characterization of dihydroartemisinin-resistant colon carcinoma HCT116/R cell line. Mol Cell Biochem 2012;360:329–37.
18. Hutter G, Sinha P. Proteomics for studying cancer cells and the development of chemoresistance. Proteomics 2001;1:1233–48.
19. Di Michele M, Della Corte A, Cicchillitti L, Del Boccio P, Urbani A, Ferlini C, et al. A proteomic approach to paclitaxel chemoresistance in ovarian cancer cell lines. Biochim Biophys Acta 2009;1794:225–36.
20. Chuthapisith S, Layfield R, Kerr ID, Hughes C, Eremin O. Proteomic profiling of MCF-7 breast cancer cells with chemoresistance to different types of anti-cancer drugs. Int J Oncol 2007;30:1545–51.
21. Cicchillitti L, Di Michele M, Urbani A, Ferlini C, Donat MB, Scambia G, et al. Comparative proteomic analysis of paclitaxel sensitive A2780 epithelial ovarian cancer cell line and its resistant counterpart A2780TC1 by 2D-DIGE: the role of ERp57. J Proteome Res 2009;8:1902–12.
22. Zhang JT, Liu Y. Use of comparative proteomics to identify potential resistance mechanisms in cancer treatment. Cancer Treat Rev 2007;33:741–56.
23. Tong A, Zhang H, Li Z, Gou L, Wang Z, Wei H, et al. Proteomic analysis of liver cancer cells treated with suberonylanilide hydroxamic acid. Cancer Chemother Pharmacol 2008;61:791–802.
24. Silva TF, Martins LM, Guedes da Silva MF, Fernandes AR, Silva A, Borralho PM, et al. Cobalt complexes bearing scorpionate ligands: synthesis, characterization, cytotoxicity and DNA cleavage. Dalton Trans 2012;41:12888–97.
25. Conde J, Larguinho M, Cordeiro A, Raposo LR, Costa PM, Santos S, et al. Gold-nanobeacons for gene therapy: evaluation of genotoxicity, cell toxicity and proteome profiling analysis. Nanotoxicology 2013; DOI:10.3109/17435390.2013.802821.
26. Borralho PM, Kren BT, Castro RE, Silva IB, Steer CJ, Rodrigues CM. MicroRNA-143 reduces viability and increases sensitivity to 5-fluorouracil in HCT116 human colorectal cancer cells. FEBS J 2009;276:6689–700.
27. Rubio S, Estevez F, Cabrera J, Reiter RJ, Loro J, Quintana J. Inhibition of proliferation and induction of apoptosis by melatonin in human myeloid HL-60 cells. J Pineal Res 2007;42:131–8.
28. Oberhammer F, Fritsch G, Schmied M, Pavelka M, Printz D, Purchio T, et al. Condensation of the chromatin at the membrane of an apoptotic nucleus is not associated with activation of an endonuclease. J Cell Sci 1993;104:317–26.
29. Venardos KM, Perkins A, Headrick J, Kaye DM. Myocardial ischemia-reperfusion injury, antioxidant enzyme systems, and selenium: a review. Curr Med Chem 2007;14:1539–49.
30. Lessor TJ, Yoo JY, Xia X, Woodford N, Hamburger AW. Ectopic expression of the ErbB-3 binding protein ebp1 inhibits growth and induces differentiation of human breast cancer cell lines. J Cell Physiol 2000;183:321–9.
31. Squatrito M, Mancino M, Donzelli M, Areces LB, Draetta GF. EBP1 is a nucleolar growth-regulating protein that is part of pre-ribosomal ribonucleoprotein complexes. Oncogene 2004;23:4454–65.
32. Hermeking H, Benzinger A. 14-3-3 proteins in cell cycle regulation. Semin Cancer Biol 2006;16:183–92.
33. Mhawech P. 14-3-3 proteins – an update. Cell Res 2005;15:228–36.

34. Rho SB, Lee JH, Park MS, Byun HJ, Kang S, Seo SS, et al. Anti-apoptotic protein TCTP controls the stability of the tumor suppressor p53. FEBS Lett 2011;585:29–35.
35. Gnanasekar M, Thirugnanam S, Zheng G, Chen A, Ramaswamy K. Gene silencing of translationally controlled tumor protein (TCTP) by siRNA inhibits cell growth and induces apoptosis of human prostate cancer cells. Int J Oncol 2009;34:1241–6.
36. Gibert B, Hadchity E, Czekalla A, Aloy MT, Colas P, Rodriguez-Lafrasse C, et al. Inhibition of heat shock protein 27 (HspB1) tumorigenic functions by peptide aptamers. Oncogene 2011;30:3672–81.
37. Hansen RK, Parra I, Lemieux P, Oesterreich S, Hilsenbeck SG, Fuqua SA. Hsp27 overexpression inhibits doxorubicin-induced apoptosis in human breast cancer cells. Breast Cancer Res Treat 1999;56:187–96.
38. Ciocca DR, Calderwood SK. Heat shock proteins in cancer: diagnostic, prognostic, predictive, and treatment implications. Cell Stress Chaperones 2005;10:86–103.
39. Reddy RK, Lu J, Lee AS. The endoplasmic reticulum chaperone glycoprotein GRP94 with Ca(2+)-binding and antiapoptotic properties is a novel proteolytic target of calpain during etoposide-induced apoptosis. J Biol Chem 1999;274:28476–83.
40. Langer R, Feith M, Siewert JR, Wester HJ, Hoefler H. Expression and clinical significance of glucose regulated proteins GRP78 (BiP) and GRP94 (GP96) in human adenocarcinomas of the esophagus. BMC Cancer 2008;8:70.
41. Wang Q, He Z, Zhang J, Wang Y, Wang T, Tong S, et al. Overexpression of endoplasmic reticulum molecular chaperone GRP94 and GRP78 in human lung cancer tissues and its significance. Cancer Detect Prev 2005;29:544–51.
42. Zheng HC, Takahashi H, Li XH, Hara T, Masuda S, Guan YF, et al. Overexpression of GRP78 and GRP94 are markers for aggressive behavior and poor prognosis in gastric carcinomas. Hum Pathol 2008;39:1042–9.
43. Olson MF, Sahai E. The actin cytoskeleton in cancer cell motility. Clin Exp Metastasis 2009;26:273–87.
44. Shoshan-Barmatz V, Keinan N, Zaid H. Uncovering the role of VDAC in the regulation of cell life and death. J Bioenerg Biomembr 2008;40:183–91.
45. McGee AM, Douglas DL, Liang Y, Hyder SM, Baines CP. The mitochondrial protein C1qbp promotes cell proliferation, migration and resistance to cell death. Cell Cycle 2011;10:4119–27.
46. Amamoto R, Yagi M, Song YH, Oda Y, Tsuneyoshi M, Naito S, et al. Mitochondrial p32/C1QBP is highly expressed in prostate cancer and is associated with shorter prostate-specific antigen relapse time after radical prostatectomy. Cancer Sci 2011;102:639–47.
47. Rabinovich GA. Galectin-1 as a potential cancer target. Br J Cancer 2005;92:1188–92.
48. Salatino M, Croci DO, Bianco GA, Ilarregui JM, Toscano MA, Rabinovich GA. Galectin-1 as a potential therapeutic target in autoimmune disorders and cancer. Expert Opin Biol Ther 2008;8:45–57.
49. Lee J. Role of cyclophilin a during oncogenesis. Arch Pharm Res 2010;33:181–7.
50. Caputo E, Maiorana L, Vasta V, Pezzino FM, Sunkara S, Wynne K, et al. Characterization of human melanoma cell lines and melanocytes by proteome analysis. Cell Cycle 2011;10:2924–36.
51. Wittenmayer N, Jandrig B, Rothkegel M, Schluter K, Arnold W, Haensch W, et al. Tumor suppressor activity of profilin requires a functional actin binding site. Mol Biol Cell 2004;15:1600–8.